Inorganic Chemistry

Article

pubs.acs.org/IC

Coordination Polymers Based on Heterohexanuclear Rare Earth Complexes: Toward Independent Luminescence Brightness and Color Tuning

François Le Natur,[†,‡] Guillaume Calvez,*[,†,‡] Carole Daiguebonne,[†,‡] Olivier Guillou,*[,†,‡] Kevin Bernot,[†,‡] James Ledoux,[†,§] Laurent Le Pollès,[†,∥] and Claire Roiland[†,⊥]

[†]Université européenne de Bretagne, Rennes, France

[‡]INSA, UMR 6226, Institut des Sciences Chimiques de Rennes, F-35708 Rennes, France

[§]INSA, UMR 6625, Institut de Recherche Mathématique de Rennes, F-35708 Rennes, France

[∥]ENSCR, UMR 6226, Institut des Sciences Chimiques de Rennes, F-35708 Rennes, France

[⊥]Université de Rennes 1, UMR 6226, Institut des Sciences Chimiques de Rennes, F-35042 Rennes, France

Supporting Information

ABSTRACT: Reactions in solvothermal conditions between hexanuclear rare earth complexes and H_2bdc, where H_2bdc symbolizes terephthalic acid, lead to a family of monodimensional coordination polymers in which hexanuclear complexes act as metallic nodes. The hexanuclear cores can be either homometallic with general chemical formula $[Ln_6O(OH)_8(NO_3)_6]^{2+}$ (Ln = Pr−Lu plus Y) or heterometallic with general chemical formula $[Ln_{6x}Ln'_{6-6x}O(OH)_8(NO_3)_6]^{2+}$ (Ln and Ln′ = Pr−Lu plus Y). Whatever the hexanuclear entity is, the resulting coordination polymer is iso-structural to $[Y_6O(OH)_8(NO_3)_2(bdc)\text{-}(Hbdc)_2{\cdot}2NO_3{\cdot}H_2bdc]_\infty$, a coordination polymer that we have previously reported. The random distribution of the lanthanide ions over the six metallic sites of the hexanuclear entities is demonstrated by ^{89}Y solid state NMR, X-ray diffraction (XRD), and luminescent measurements. The luminescent and colorimetric properties of selected compounds that belong to this family have been studied. These studies demonstrate that some of these compounds exhibit very promising optical properties and that there are two ways of modulating the luminescent properties: (i) playing with the composition of the heterohexanuclear entities or (ii) playing with the relative ratio between two different hexanuclear entities. This enables the independent tuning of luminescence intensity and color.

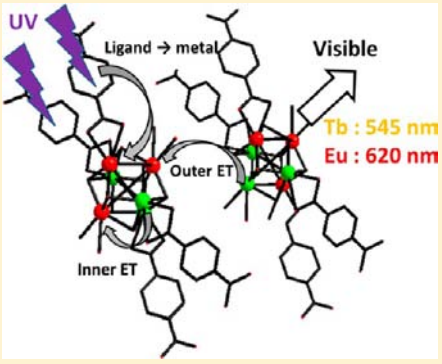

INTRODUCTION

For more than a decade, lanthanide-based coordination polymers have attracted great attention because of their ability to provide potentially porous materials[1,2] and their interesting luminescent properties.[3−6] Most of the reported works devoted to lanthanide-based coordination polymers focus on the optimization of the choice of the ligand.[7] However, very few works deal with the optimization of the metallic centers. Indeed, although the validity of the approach has been demonstrated for transition metal ions,[8−11] there are only few lanthanide containing coordination polymers in which polynuclear complexes act as metallic centers.

Actually, polynuclear lanthanide complexes have been known for more than 20 years,[12,13] and since the pioneering work of Unfried et al.[14−20] numerous such entities have been reported[21−25] ranging from tetranuclear[26] to pentadecanuclear entities.[27] Unfortunately most of these complexes were quite unstable and could not be used as molecular precursors for the design of supramolecular frameworks. Additionally, most of the polynuclear rare earth-based coordination polymers reported to date[26,28−37] have been prepared via self-assembly processes by using lanthanide oxides or salts as starting materials. This makes difficult the rational tailoring of their physical properties. For almost a decade our group has been involved in the synthesis and characterization of hexanuclear rare earth complexes with general chemical formula $[Ln_6O(OH)_8(NO_3)_6]^{2+}$ usable as stable molecular building blocks[38−42] (Figure 1).

Recently, we succeeded in synthesizing a family of homohexanuclear-based coordination polymers from isolated homohexanuclear complexes.[41] These compounds have general chemical formula $\{[Ln_6O(OH)_8](NO_3)_2(bdc)\text{-}(Hbdc)_2{\cdot}2NO_3{\cdot}H_2bdc\}_\infty$ where H_2bdc symbolizes terephthalic acid (1,4-benzene-dicarboxylic acid). Their X-ray powder crystal structure is monodimensional and can be described as the juxtaposition of molecular chain-like motifs spreading along the $\vec{a} + \vec{c}$ direction (CCDC-784583[43,44]). One molecule of terephthalic acid and two nitrate ions per asymmetric unit lie in

Received: April 8, 2013
Published: May 21, 2013

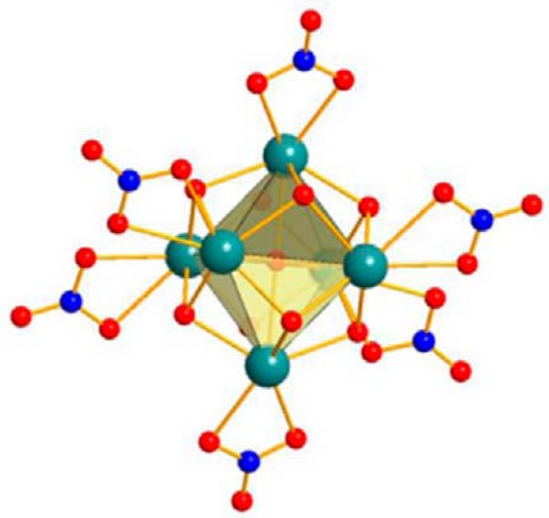

Figure 1. Hexanuclear complex $[Ln_6O(OH)_8(NO_3)_6]^{2+}$.

the interchain space (Figure 2). Intermetallic distances inside a given hexanuclear complex are very short and lie in the 2.9−4.2 Å range. On the other hand the hexanuclear entities are rather far from each other: The shortest distances between Ln(III) ions that belong to different hexanuclear entities are found between 7.6 Å and 9.9 Å (Supporting Information, Tables S1 and S2). These structural features are promising as far as optical properties are concerned. Actually one can expect intense intermetallic energy transfer inside a given hexanuclear entity and weaker intermetallic energy transfer between neighboring hexanuclear entities (above a 10 Å intermetallic distance it is commonly admitted that intermetallic energy transfer is weak[45,46]). Moreover, the terephthalate ligand is well-known for its good sensitization efficiency for lanthanide ions.[47,48]

Therefore we have decided to undertake the study of the luminescent properties of this family of compounds. In this paper we report the syntheses, characterization, and luminescent properties of two coordination polymers based on homohexanuclear compounds, $\{[Eu_6O(OH)_8](NO_3)_2(bdc)(Hbdc)_2{\cdot}2NO_3{\cdot}H_2bdc\}_\infty$ and $\{[Tb_6O(OH)_8](NO_3)_2(bdc)(Hbdc)_2{\cdot}2NO_3{\cdot}H_2bdc\}_\infty$ and two series of heterohexanuclear-based compounds with general chemical formulas $\{[Tb_{6x}Y_{6-6x}O(OH)_8](NO_3)_2(bdc)(Hbdc)_2{\cdot}2NO_3{\cdot}H_2bdc\}_\infty$ and $\{[Tb_{6x}Eu_{6-6x}O(OH)_8](NO_3)_2(bdc)(Hbdc)_2{\cdot}2NO_3{\cdot}H_2bdc\}_\infty$ hereafter symbolized by $\{\mathbf{Eu_6}\}_\infty$, $\{\mathbf{Tb_6}\}_\infty$, $\{\mathbf{Tb_{6x}Y_{6-6x}}\}_\infty$, and $\{\mathbf{Tb_{6x}Eu_{6-6x}}\}_\infty$, respectively.

EXPERIMENTAL SECTION

Synthesis of the Microcrystalline Powders. Benzene-1,4-dicarboxylic acid was purchased from Acros Organics and used without further purification. Anhydrous acetonitrile was purchased from Acros Organics and kept on molecular sieves. Hydrated lanthanide oxides were purchased from Strem chemicals. Lanthanide nitrates were synthesized according to established procedures.[49] Then homohexanuclear complexes were synthesized according to procedures that have already been described.[40,42] Heterohexanuclear complexes' synthesis is similar to that of homohexanuclear complexes. The only difference is that the starting solution is an aqueous solution of a mixture of lanthanide nitrates instead of an aqueous solution of a pure lanthanide nitrate.

0.05 mmol of hexanuclear complexes, 0.25 mmol of H_2bdc, and 3 mL of dry acetonitrile have been put in 24 mL Paar autoclaves. Mixtures have been heated at 130 °C for 50 h and then allowed to cool down at a cooling rate of 1 °C h^{-1}. The resulting solids have been filtered and dried under Ar. The yields of the syntheses are roughly 90% regarding the hexanuclear complex. Iso-structurality of all these compounds has been assumed on the basis of their X-ray diffraction patterns (Figure 3).

Elemental chemical analyzes were performed for homohexanuclear-based compounds only. The results are in perfect agreement with what has been reported previously.[40] For heterohexanuclear-based compounds the relative ratios between the two different lanthanide ions have been measured by EDS. The results are listed in Table 1. Reproducibility has been carefully checked by measuring several times for each sample. These measurements show good agreement between theoretical and experimental values. This can be related to the ionic radii of the involved lanthanide ions that are close.

X-ray Powder Diffraction. The diagrams have been collected using a Panalytical X'Pert Pro diffractometer with an X'Celerator detector. The typical recording conditions were 40 kV, 40 mA for Cu−Kα (λ = 1.542 Å), the diagrams were recorded in θ/θ mode in 60 min between 5° and 75° (8378 measurements) with a step size of 0.0084° and a scan time of 50 s. The calculated patterns were produced using the Powdercell and WinPLOTR software programs.[50−52] For Pattern

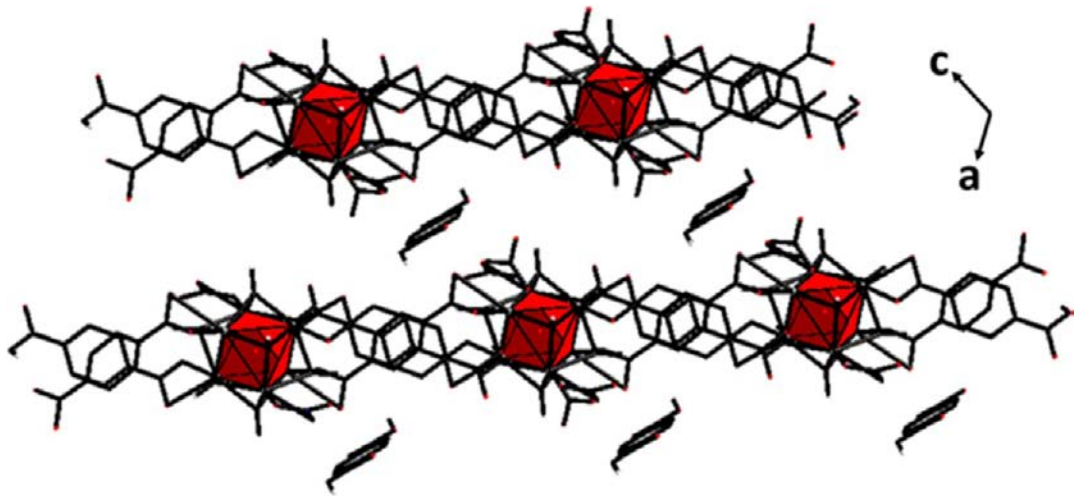

Figure 2. Projection view along the $\vec{b}$ axis of $\{[Y_6O(OH)_8](NO_3)_2(bdc)(Hbdc)_2{\cdot}2NO_3{\cdot}H_2bdc\}_\infty$. Hexanuclear octahedrons have been drawn. This compound crystallizes in the triclinic system, space group $P\bar{1}$ (no. 2) with a = 10.4956(6) Å, b = 11.529(2) Å, c = 12.357(2) Å, α = 86.869(9)°, β = 114.272(6)°, γ = 71.624(7)°, V = 1264.02 Å^3, and Z =2.[41].

dx.doi.org/10.1021/ic4008697 | Inorg. Chem. 2013, 52, 6720−6730

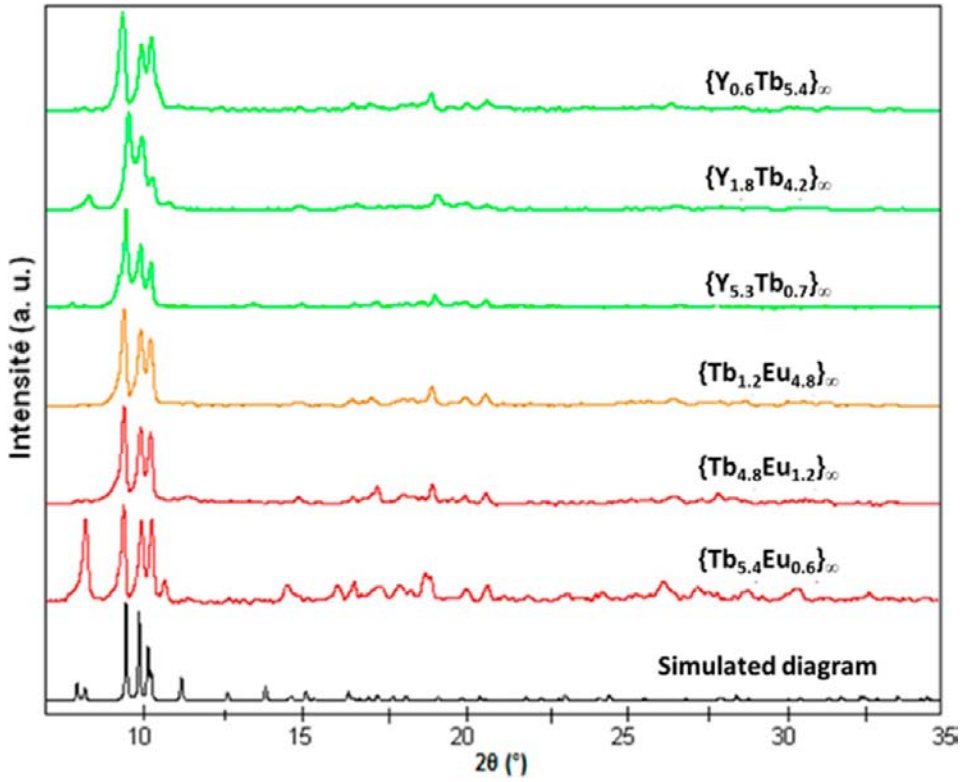

Figure 3. Experimental X-ray diffraction diagrams of some heterohexanuclear-based compounds and simulated X-ray diffraction diagrams of $\{[Y_6O(OH)_8](NO_3)_2(bdc)(Hbdc)_2{\cdot}2NO_3{\cdot}H_2bdc\}_\infty$.

Table 1. Relative Ratios between Ln and Ln′ for Compounds of the Series $\{Ln_{6x}Ln'_{6-6x}\}_\infty$ with Ln = Tb, Ln′ = Eu or Y, and $0 \leq x \leq 1$

$\{Tb_{6x}Y_{6-6x}\}_\infty$			$\{Tb_{6x}Eu_{6-6x}\}_\infty$		
Tb (%)[a]	Y (%)[a]	x[b]	Tb (%)[a]	Eu (%)[a]	x[b]
100	0	1.00	100	0	1
93(2)	7(2)	0.90	97(2)	3(2)	0.95
68(2)	32(2)	0.70	92(2)	8(2)	0.90
63(2)	37(2)	0.60	82(2)	18(2)	0.80
42(2)	58(2)	0.40	47(2)	53(2)	0.50
33(2)	67(2)	0.30	21(2)	79(2)	0.20
10(2)	90(2)	0.10	0	100	0
0	100	0			

[a]Experimental values (metal fractions used during the syntheses). [b]Theoretical values (metal fractions found by element analyses).

indexing, the extractions of the peak positions were carried out via the WinPLOTR software. The pattern indexing was performed by the program McMaille,[53] and the refinement of the unit-cell parameters by means of the Chekcell program which is a modified version of Cellref from the CRYSFIRE suite.[54]

^{89}Y NMR-MAS Measurements. Solid state ^{89}Y NMR-MAS measurements have been performed for heterohexanuclear complexes with various Y^{3+}/Lu^{3+} ratios using a Bruker Avance III spectrometer equipped with a 14.1 T magnet giving a Larmor Frequency of 29.4 MHz for ^{89}Y. Samples were packed into 7 mm rotors rotated at a spinning rate of 4 kHz. ^{89}Y MAS NMR spectra were acquired using cross-polarization (CP) from ^{1}H using a contact time of 5 ms (ramped for ^{1}H), SPINAL64 ^{1}H decoupling during acquisition with an rf field strength of ~60 kHz and recycle interval of 3 s. Chemical shift scales are shown relative to 1 M YCl_3 in aqueous solution.

FT-IR Measurements. FT-IR measurements have been performed on KBr pellets between 400 cm^{-1} and 4000 cm^{-1} using a Perkin-Elmer Paragon 1000 PC spectrometer. All compounds exhibit similar spectra. These spectra clearly show the characteristic bands for both protonated and deprotonated carboxylato groups, that is, 1410 cm^{-1} and 1380 cm^{-1} for −COOH and $-COO^-$, respectively. The characteristic band for nitrate at 1340 cm^{-1} is also observed. On the other hand, the spectra do not show any characteristic band for either water molecules or nitrile functions.

Energy Dispersive Spectroscopy. All EDS measurements were carried out with a Hitachi TM-1000, Tabletop Microscope version 02.11 (Hitachi High-Technologies Corporation, Tokyo, Japan) with EDS analysis system (SwiftED-TM, Oxford Instruments Link INCA). The detector is a Silicon drift detector, with an energy resolution of 165 eV which allows us to detect the element from Na to U. With the software SwiftED-TM, qualitative and quantitative analyses can be performed. All the samples have been observed by means of an electron beam accelerated at 15 kV, under high vacuum. The samples were assembled on carbon discs, stuck on an aluminum stub fixed at 7 mm from EDX beam, with an angle of measurement of 22°.

Solid State Luminescent Measurements. Solid state emission spectra were measured on a Horiba Jobin-Yvon Fluorolog III fluorescence spectrometer with a pulse Xe lamp. Slit widths for excitation and emission were 2 nm.

Solid state luminescence spectra were all recorded at room temperature between 450 and 800 nm in identical operating conditions without turning the lamp off to ensure a valid comparison between the emission spectra. Reproducibility of the measurements has been carefully checked by reproducing several times. The data were collected at every nm with an integration time of 100 ms for each step. The quantum yield measurements were performed using a Jobin-Yvon integrating sphere ($\Phi = (E_c - E_a)/(L_a - L_c)$ with E_c the emission spectrum of the sample, E_a the "blank" emission spectrum, L_a the "blank" absorption, and L_c the sample absorption around excitation wavelength). It must be noticed that, because of their low stability, some samples have been protected by glycerol.

Luminescence intensities of the samples expressed in Cd m^{-2} have been measured with a Gigahertz-Optik X1-1 optometer with an

dx.doi.org/10.1021/ic4008697 | Inorg. Chem. 2013, 52, 6720−6730

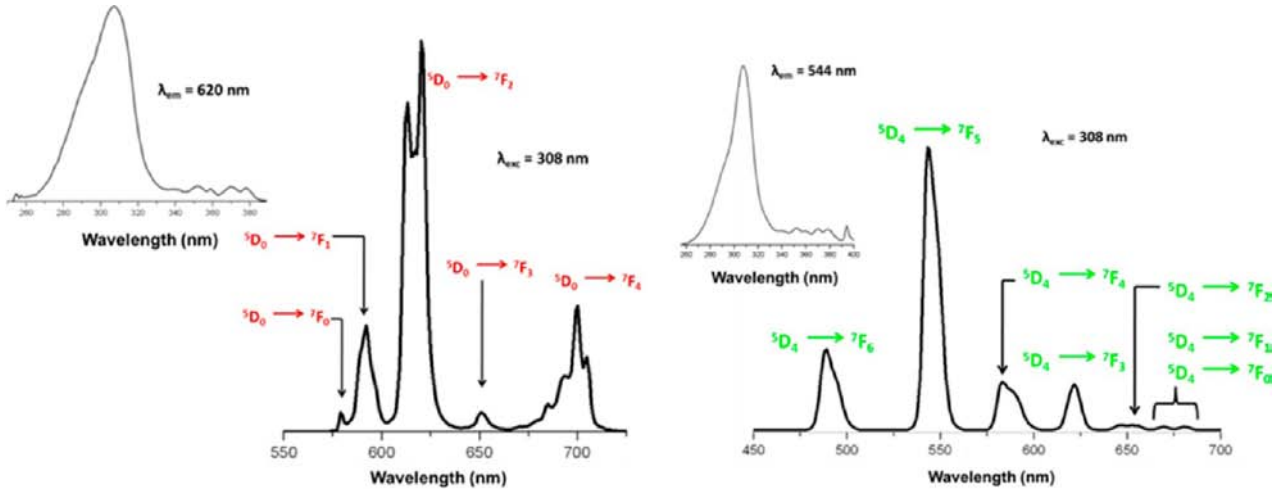

Figure 4. Excitation (in inset) and luminescence spectra of $\{\mathbf{Eu_6}\}_\infty$ (left) and $\{\mathbf{Tb_6}\}_\infty$ (right).

integration time of 200 ms on 1.5 cm^2 in area pellets. The intensity of the UV flux, 2.5(1) W m^{-2}, was measured with a Vilber Lourmat VLX-3W radiometer.

Colorimetric Measurements. The CIE (Commission Internationale de l'Eclairage) (*x*,*y*) emission color coordinates[55,56] were obtained using a MSU-003 colorimeter (Majantys) with the PhotonProbe 1.6.0 Software (Majantys). Color measurements: 2°, CIE 1931, step 5 nm, under 312 nm UV light. $X = k \times \int_{380nm}^{780nm} I_\lambda \times x_\lambda$, $Y = k \times \int_{380nm}^{780nm} I_\lambda \times y_\lambda$, and $Z = k \times \int_{380nm}^{780nm} I_\lambda \times z_\lambda$ with k constant for the measurement system, I_λ sample spectrum intensity, wavelength depending, x_λ, y_λ, z_λ trichromatic values $x = X/(X + Y + Z)$, $y = Y/(X + Y + Z)$, and $z = Z/(X + Y + Z)$. Mean *xyz* values are given for each sample, which act as light sources (luminescent samples). Standards from Phosphor Technology used, calibrated at 312 nm: red phosphor Gd_2O_2S:Eu ($x = 0.667$, $y = 0.330$) and green phosphor Gd_2O_2S:Tb ($x = 0.328$, $y = 0.537$)

RESULTS AND DISCUSSION

Homohexanuclear Complexes-Based Coordination Polymers. For several years our group has been involved in the study of lanthanide-based coordination polymers that exhibit interesting porosity[57−59] or luminescent properties.[60,61] In this framework, some coordination polymers that involve benzene-poly carboxylate as ligands[62] have been studied. Some of these systems,[63] and especially those constructed from terephthalate have retained our attention because of their promising luminescent properties.[47,48,64] To estimate the potentiality of the hexanuclear complexes-based coordination polymers we have decided to investigate the luminescent properties of the compounds that involve Eu^{3+} or Tb^{3+}: $\{\mathbf{Eu_6}\}_\infty$ and $\{\mathbf{Tb_6}\}_\infty$. The excitation spectra of these compounds present a maximum around 308 nm. Actually, upon excitation of the conjugated organic ligand, intersystem crossing and energy transfer occur and lead to lanthanide ion luminescence. This well-known phenomenon is referred to as the "antenna effect".[3,4,65−67] These compounds under UV irradiation (λ_{exc} = 308 nm) exhibit strong red and green luminescence with 20(2)% and 59(5)% quantum yields respectively (Figure 4). The luminescence decay rates of these two compounds are monoexponential.

The emission spectrum of the Eu^{3+}-containing compound shows five emission peaks at 579 nm, 591 nm, 620 nm, 650 nm, and 700 nm that correspond to $^5D_0 \rightarrow {}^7F_J$ with J = 0−4 transitions. It is dominated by the $^5D_0 \rightarrow {}^7F_2$ transition. The emission spectrum of the Tb^{3+}-containing compound shows seven emission peaks at 489 nm, 544 nm, 584 nm, 621 nm, 650 nm, 671 nm, and 683 nm that correspond to $^5D_4 \rightarrow {}^7F_J$ with J = 6−0 transitions. It is dominated by the $^5D_4 \rightarrow {}^7F_5$ transition. Spectroscopic and colorimetric results for both compounds are listed in Table 2.

Table 2. Spectroscopic and Colorimetric Measurements for $\{\mathbf{Ln_6}\}_\infty$ with Ln = Eu or Tb

Ln	Φ (%)	τ_{obs} (ms)	*x*	*y*	luminance[a]
Eu	20(2)	0.41(4)	0.66(1)	0.34(1)	35(3)
Tb	59(5)	1.40(5)	0.33(1)	0.59(1)	74(7)

[a]The values are expressed in Cd m^{-2} and represent the luminous flux weighted by the spectral response of human eye.

The very high quantum yields observed for both compounds are very promising. Actually, considering the very short intermetallic distances inside the hexanuclear entities one could expect strong intermetallic energy transfer (hereafter referenced as "inner energy transfer") between lanthanide ions that belong to the same hexanuclear entity. Therefore, as already observed in "classical" lanthanide-based coordination polymers,[68] it should be possible to enlarge the intermetallic distance and to enhance the quantum yields by diluting optically active rare earth ions by inactive ones. However, in contrast with "classical" lanthanide-based coordination polymers, there is a second intermetallic energy transfer which is less efficient than the former (hereafter referenced as "outer energy transfer"). It involves lanthanide ions that belong to different hexanuclear entities (See Scheme 1).

Heterohexanuclear Complexes. Heterohexanuclear complexes with general chemical formula $[Tb_{6x}Y_{6-6x}O(OH)_8(NO_3)_6]^{2+}$ with $0 \leq x \leq 1$ hereafter symbolized as $[\mathbf{Tb_{6x}Y_{6-6x}}]^{2+}$ have been prepared. Analysis of their powder X-ray diffraction patterns indicates that there is no long-range order nor segregation in these compounds.[47] Actually, the powder X-ray diffraction patterns show neither overstructure peaks nor splitting of the diffraction peaks. As a matter of example, the powder X-ray diffraction diagrams of four samples are reported in Figure 5. All the other series of heterohexanuclear complexes exhibit similar behaviors.

Recent papers prove that ^{89}Y NMR is a useful probe of local ordering in solid state compounds.[69−72] Therefore, to verify

dx.doi.org/10.1021/ic4008697 | Inorg. Chem. 2013, 52, 6720−6730

Scheme 1. Schematic Representation of the Two Different Intermetallic Energy Transfer Pathways (Inner and Outer Energy Transfers)

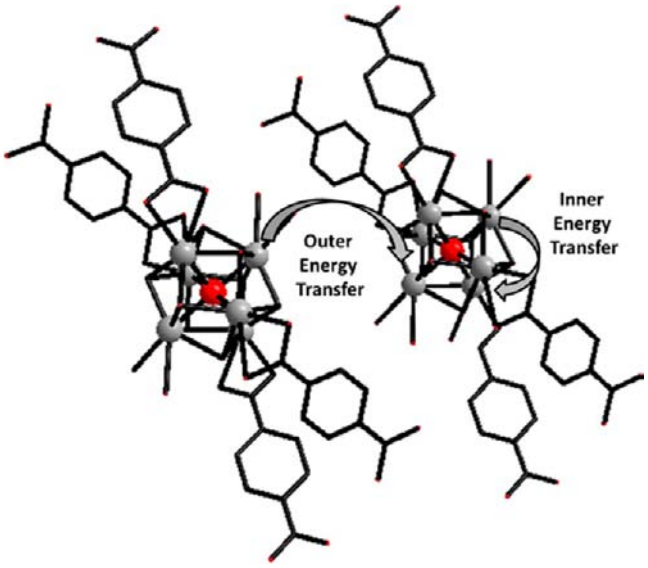

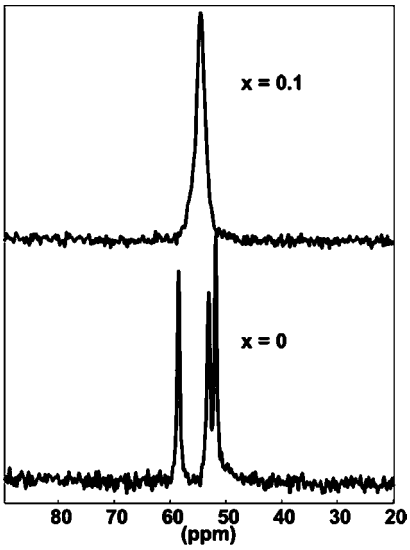

Figure 6. ^{89}Y CPMAS NMR spectra of $[Y_6]^{2+}$ (Bottom) and of $[Y_{6-6x}Lu_{6x}]^{2+}$ with x = 0.1 (Top). For $[Y_6]^{2+}$ chemical shifts are δ_1 = 51.7 ppm, δ_2 = 53.0 ppm, and δ_3 = 58.4 ppm.

that the hexanuclear cores are themselves heterometallic, we have performed solid state ^{89}Y CPMAS NMR measurements on a series of $[Y_{6-6x}Lu_{6x}]^{2+}$ complexes. Diamagnetic lanthanide ions have been chosen for achieving high resolution NMR solid state experiments. These measurements show no evidence for local ordering and support the interpretation of randomly distributed yttrium and lutetium ions over the six metallic sites of the hexanuclear entities (Figure 6).

The solid state ^{89}Y CPMAS NMR spectrum of $[Y_6]^{2+}$ is consistent with the crystal structure that actually presents three crystallographically inequivalent and equally populated Y^{3+} positions.[40] The spectrum of $[Y_{6-6x}Lu_{6x}]^{2+}$ with x = 0.1 is very different from the spectrum recorded on the yttrium pure sample and clearly support the assumption of randomly distributed lanthanide ions. However it is more difficult to interpret. This was expected because the random distribution of the lanthanide ions implies the coexistence of several different hexanuclear species (Scheme 2).

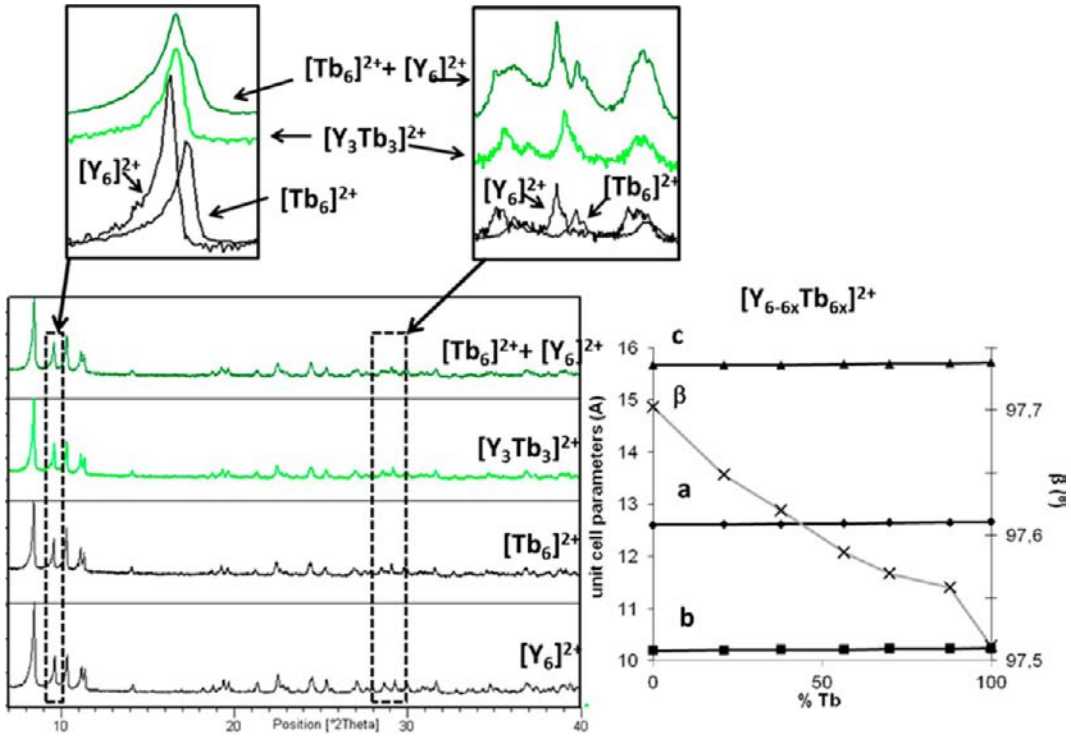

Figure 5. Left: Powder X-ray diffraction patterns of $[Y_6]^{2+}$, $[Tb_6]^{2+}$, $[Y_3Tb_3]^{2+}$ and of a fifty/fifty mixture of $[Y_6]^{2+}$ and $[Tb_6]^{2+}$. Right: Fitted cell parameters versus Tb(III) content (in atom percent) for $[Tb_{6x}Y_{6-6x}]^{2+}$ compounds.

dx.doi.org/10.1021/ic4008697 | Inorg. Chem. 2013, 52, 6720−6730

Scheme 2. Possible Distributions of Two Different Lanthanide Ions[a] over the Six Metallic Sites in Hetero-Hexanuclear Complexes[b]

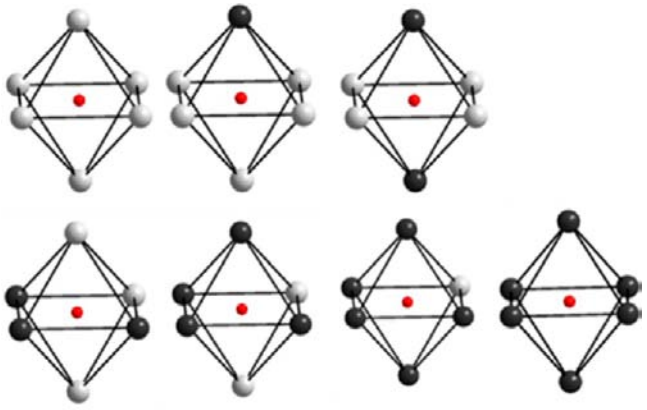

[a]Symbolized by dark and light grey balls respectively.

[b]Red balls indicate μ_6-O atoms.

It is possible to calculate the population of each species versus the overall composition of the heterohexanuclear complexes, assuming that the difference between ionic radii does not induce any deformation of the polyhedron. This assumption implies that (i) the octahedron is perfectly regular, and (ii) rare earth ions present the same affinity for each metallic site. These assumptions are obviously not true but seem realistic.

In that setting, the probability $\mathbb{P}\{C(i)\}$ of obtaining the configuration $C(i)$ with chemical formula $[Ln_iLn'_{6-i}O(OH)_8(NO_3)_2]^{2+}$ is

$$\mathbb{P}\{C(i)\} = \frac{C^i_{n_{Ln}} C^{6-i}_{n_{Ln'}}}{C^6_n}$$

with $C^k_n = (n!)/((n-k))!k!)$ and where n_{Ln} and $n_{Ln'}$ are respectively the numbers of Ln and Ln′ ions in solution and n the total number of lanthanide ions in solution.[73] As a matter of example, the relative abundance of the different hexanuclear complexes obtained from an equimolar mixture is calculated in Scheme 3.

These calculations support the experimental ^{89}Y NMR results. Indeed, the complicated patterns of the spectra are justified by the important number of different hexanuclear complexes. All these results strongly suggest that the lanthanide ions are randomly distributed over the different metallic sites of the crystal structure. To date, and despite great efforts, it has not been possible to further correlate experimental results and calculations. Our group is working along this line.

Scheme 3. Relative Abundance of the Different Hexa-Nuclear Complexes Obtained from an Equimolar Mixture of Ln and Ln′ Ions ($n = 10^{20}$)[a]

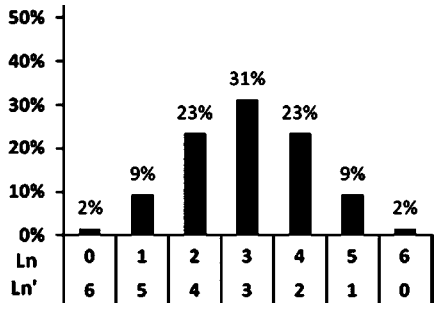

[a]For other mixtures see Supporting Information, Figure S1.

Heterohexanuclear Complexes-Based Coordination Polymers. Heterohexanuclear complexes have been used as molecular bridging blocks for the syntheses of heterohexanuclear complexes-based coordination polymers. Therefore, as a first approach, it is possible to consider that these compounds could be described on the basis of heterohexanuclear entities with statistically identical compositions. Because of the very short intermetallic distances between lanthanide ions that belong to the same hexanuclear complex, intermetallic deactivation must be dominant inside the homonuclear complexes. Therefore, it should be possible to increase the mean distance between optically active lanthanide ions by randomly introducing optically nonactive ones. We have thus decided to investigate the luminescent properties of the compounds $\{\mathbf{Y_{6x}Tb_{6-6x}}\}_\infty$ (Figure 7).

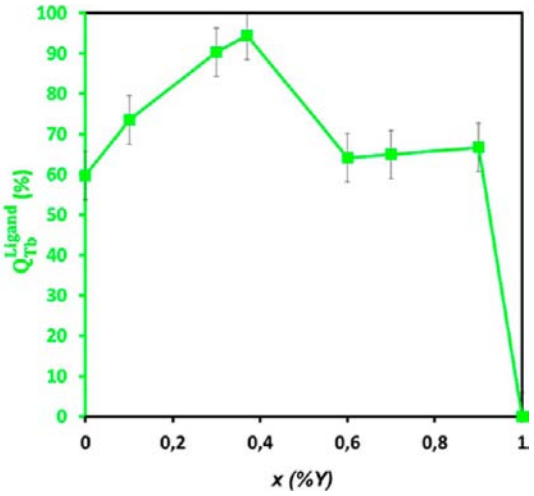

Figure 7. Overall quantum yield of Tb(III) luminescence Q^{Ligand}_{Tb} versus Y(III) content in $\{\mathbf{Y_{6x}Tb_{6-6x}}\}_\infty$.

As expected, the dilution of the Tb(III) ions by the addition of Y(III) ions reduces the inner Tb(III)-to-Tb(III) energy transfer and the overall quantum yield strongly increases and reaches values close to 100%. Then, when the Tb(III) content becomes too low, the quantum yield diminishes. However, whatever the Y(III) content is, the Tb(III) overall quantum yield remains at least as high as the one observed for $\{\mathbf{Tb_6}\}_\infty$. Colorimetric coordinates and luminance have also been measured. Results are reported in Table 3.

From these results it can first be noticed that the dilution effect on the enhancement of the overall quantum yield is more pronounced in these compounds than in "classical" lanthanide-based coordination polymers.[68,74] On the other hand, in contrast with what is observed for "classical" lanthanide-based coordination polymers, dilution seems to have no effect upon luminescence color (x,y) and brightness (luminance). This feature, which can probably be related to the very short intermetallic distances that are observed in hexanuclear complexes, is of great interest as far as technological applications are targeted. Indeed, these data show that it is possible to design systems containing only a few percent of

dx.doi.org/10.1021/ic4008697 | Inorg. Chem. 2013, 52, 6720−6730

Table 3. Spectroscopic and Colorimetric Results for Compounds That Belong to the Series $\{Y_{6x}Tb_{6-6x}\}_\infty$

	spectroscopy		colorimetry		luminance[a]
	Φ (%)	τ_0 (ms)	x	y	(Cd m^{-2})
$\{Tb_6\}_\infty$	59 (5)	1.40 (5)	0.33 (1)	0.59 (1)	74 (7)
$\{Y_{0.6}Tb_{5.4}\}_\infty$	73 (7)	1.37 (5)	0.33 (1)	0.56 (1)	71 (7)
$\{Y_{1.8}Tb_{4.2}\}_\infty$	90 (7)	1.41 (5)	0.34 (1)	0.58 (1)	68 (6)
$\{Y_{2.4}Tb_{3.6}\}_\infty$	94 (7)	1.41 (5)	0.34 (1)	0.54 (1)	74 (7)
$\{Y_{3.6}Tb_{2.4}\}_\infty$	64 (5)	1.40 (5)	0.35 (1)	0.57 (1)	71 (7)
$\{Y_{4.2}Tb_{1.8}\}_\infty$	65 (5)	1.41 (5)	0.35(1)	0.58 (1)	72 (7)
$\{Y_{5.4}Tb_{0.6}\}_\infty$	67 (5)	1.39 (5)	0.34 (1)	0.51(1)	74 (7)

[a]The values are expressed in Cd m^{-2} and represent the luminous flux weighted by the spectral response of human eye.

Tb^{3+} and exhibiting luminescent properties close to those of the homologous homonuclear Tb-containing system. Moreover, yttrium is less expensive than terbium.

On the basis of these results, we have undertaken the study of compounds with general chemical formula $\{Tb_{6x}Eu_{6-6x}\}_\infty$. The green Tb(III) emission and the red Eu(III) emission have been studied independently. The luminescent contributions to the total emission spectra of the Eu(III) ions and of the Tb(III) ions have been estimated on the basis of the $^5D_0 \rightarrow {}^7F_0$ and $^5D_4 \rightarrow {}^7F_5$ transitions, respectively, because they do not overlap with other transitions. Since all compounds are isostructural and the metallic ions are perfectly randomly distributed, we have assumed that the relative intensities of the different peaks are similar to the ones observed in the corresponding homonuclear compounds. Results are listed in Table 4. As it

Table 4. Overall Quantum Yields and Lifetimes for Compounds That Belong to the Series $\{Tb_{6x}Eu_{6-6x}\}_\infty$

	Eu^{3+}		Tb^{3+}	
	τ_{obs} (ms)	Q_{Eu}^{Ligand} (%)	τ_{obs} (ms)	Q_{Tb}^{Ligand} (%)
$\{Eu_6\}_\infty$	0.41 (4)	20 (2)		
$\{Tb_{1.2}Eu_{4.8}\}_\infty$	0.96 (9)[a]	22 (2)		
$\{Tb_{3.0}Eu_{3.0}\}_\infty$	0.61 (6)	25 (2)	0.38 (4)	0.5 (1)
$\{Tb_{4.8}Eu_{1.2}\}_\infty$	1.12 (5)[a]	53 (5)		2.0 (2)
$\{Tb_{5.4}Eu_{0.6}\}_\infty$	1.13 (5)[a]	52 (5)		3.0 (3)
$\{Tb_{5.7}Eu_{0.3}\}_\infty$	0.69 (4)	12 (1)	0.38 (4)	3.3 (3)
$\{Tb_6\}_\infty$			1.40 (5)	59 (5)

[a]Samples were protected by glycerol.

can be seen from Figure 8, the inner intermetallic energy transfer Tb(III)-to-Eu(III) is very efficient and the overall quantum yield for Eu(III) is strongly enhanced by Tb(III) insertion. When the Tb(III) content reaches 80%, that is, roughly 5 Tb(III) for 1 Eu(III), the Eu(III) quantum yield goes over 50%.

The yield of this Tb(III)-to-Eu(III) energy transfer (η_{ET}) can be estimated by using the relation

$$\eta_{ET} = 1 - \frac{\tau_{obs}}{\tau_0}$$

where τ_{obs} and τ_0 are respectively the lifetimes with and without an acceptor.[4] The Y^{3+} ion with its first excited levels above the luminescent levels of the Tb^{3+} ion and above the ligand triplet state cannot act as an acceptor. Therefore, replacing Eu^{3+} ions by Y^{3+} ions it is possible to measure τ_0 and therefore to calculate η_{ET}. Since in these compounds, τ_{obs} does not vary significantly with dilution the calculation has been performed for $\{Tb_3Eu_3\}_\infty$ and leads to η_{ET} = 73%. These calculations

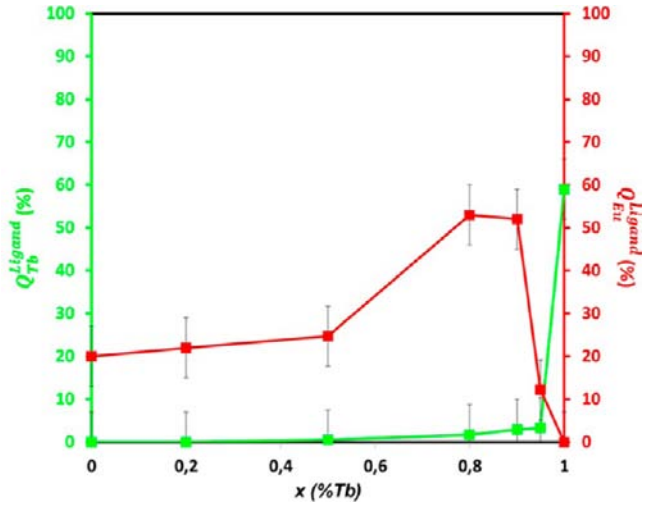

Figure 8. Overall quantum yields Q_{Eu}^{Ligand} (in red) and Q_{Tb}^{Ligand} (in green) versus the Tb(III) content for compounds that belong to the series $\{Tb_{6x}Eu_{6-6x}\}_\infty$.

confirm that the Tb(III)-to-Eu(III) inner energy transfer is efficient.

Colorimetric coordinates and luminance have also been measured. The results are listed in Table 5.

Table 5. Colorimetric and Luminance Data for Compound That Belong to the Series $\{Tb_{6x}Eu_{6-6x}\}_\infty$

	x	y	luminance[a]
$\{Eu_6\}_\infty$	0.66 (1)	0.33 (1)	35 (3)
$\{Tb_{1.2}Eu_{4.8}\}_\infty$	0.60 (1)	0.33 (1)	40 (4)
$\{Tb_{3.0}Eu_{3.0}\}_\infty$	0.65 (1)	0.34 (1)	34 (3)
$\{Tb_{4.8}Eu_{1.2}\}_\infty$	0.58 (1)	0.38 (1)	44 (4)
$\{Tb_{5.4}Eu_{0.6}\}_\infty$	0.59 (1)	0.36 (1)	44 (4)
$\{Tb_{5.7}Eu_{0.3}\}_\infty$	0.52 (1)	0.44 (1)	36 (3)
$\{Tb_6\}_\infty$	0.33 (1)	0.58 (1)	74 (7)

[a]The values are expressed in Cd m^{-2} and represent the luminous flux weighted by the spectral response of human eye.

These results indicate that in this family of compounds, inner intermetallic energy transfer mechanisms are very important. Controlling them, it is possible to obtain quite highly luminescent compounds. However, inner intermetallic energy transfers are so efficient that they limit the tuning of the luminescence color. Actually, as soon as the Eu(III) content becomes greater than 5% in the $\{Tb_{6x}Eu_{6-6x}\}_\infty$ series, the Tb(III) green luminescence becomes negligible. For low Eu^{3+} concentration it is thus possible to tune the color emission

dx.doi.org/10.1021/ic4008697 | Inorg. Chem. 2013, 52, 6720−6730

without affecting the luminance too much. Over 10% of Eu^{3+} the color remains almost unchanged (red emission).

However, as the hexanuclear entities are rather far from each other in the crystal structure, it should be possible to tune the color emission by additive color synthesis using several different hexanuclear complexes as molecular building blocks. To verify this hypothesis, we have prepared three different microcrystalline powders as schematized in Scheme 4: (i) The first one is a 50/50% mixture of $\{\mathbf{Eu_6}\}_\infty$ and $\{\mathbf{Tb_6}\}_\infty$ that have been synthesized separately. (ii) The second one is a monophasic microcrystalline powder with chemical formula $\{\mathbf{Eu_3Tb_3}\}_\infty$. (iii) The third one is a monophasic microcrystalline powder with chemical formula $\{[Eu_6O(OH)_8(NO_3)_2]_{1/2}[Tb_6O(OH)_8(NO_3)_2]_{1/2}(bdc)(Hbdc)_2{\cdot}2NO_3{\cdot}H_2bdc\}_\infty$ hereafter symbolized by $\{[\mathbf{Eu_6}]_{1/2}[\mathbf{Tb_6}]_{1/2}\}_\infty$. This sample has been prepared by reacting a 50/50 mixture of $[\mathbf{Eu_6}]^{2+}$ and $[\mathbf{Tb_6}]^{2+}$ with terephthalic acid under solvothermal conditions.

These three samples present exactly the same chemical composition and almost identical powder X-ray diffraction patterns because ionic radii of Eu^{3+} and Tb^{3+} are very close to each other (See Supporting Information, Figure S2). However, their luminescence properties are different. Emission spectra of these three samples are reported in Figure 9.

Scheme 4. Schematized Preparation of the Three Microcrystalline Powders[a]

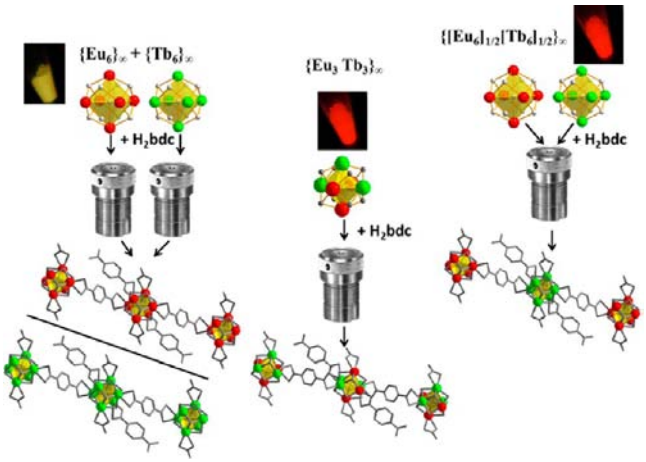

[a]In inset, pictures of the powder under UV irradiation (λ_{exc} = 312 nm).

The emission spectrum of the first sample is a perfect superimposition of the emission spectra of $\{\mathbf{Eu_6}\}_\infty$ and $\{\mathbf{Tb_6}\}_\infty$ (See Figure 4). The emission spectrum of the second sample is dominated by the red emission of Eu(III). This is in agreement with what has been described above: The efficiency of the Tb(III)-to-Eu(III) inner energy transfer inside the hexanuclear complexes is so high that the green emission of Tb(III) almost disappears (See Scheme 5).

The emission spectrum of the third sample is more unexpected. Emission spectra of both Eu(III)- and Tb(III)-based hexanuclear complexes are clearly identifiable. However, the overall spectrum is dominated by the luminescence of the Eu(III)-based hexanuclear complex, and the luminescence color of this sample is close to the luminescence color of the second sample. This indicates that in these compounds, the hexanuclear entities are actually not sufficiently isolated and some intermetallic outer energy transfer occurs between adjacent hexanuclear complexes. This is not surprising because the shortest distances between lanthanide ions that belong to neighboring hexanuclear complexes are smaller than 10 Å.

Toward Independent Tuning of Color and Luminescence. In this family of compounds two different ways of tuning the luminescence color and brightness coexist. Actually, it is possible to play with the composition of the hexanuclear complexes themselves and/or to play with a controlled mixture of different hexanuclear entities inside the solid. These two ways are quite independent from each other. To illustrate this unique feature we have decided to synthesize a compound that contains two isolated optically active hexanuclear units. A detailed analysis of the crystal structure shows that each hexanuclear unit is surrounded by 10 other hexanuclear units (See Scheme 6) that contain lanthanide ions less than 10 Å away from lanthanide ions that form the central hexanuclear complex. Therefore, an efficient optical dilution is ensured by incorporating 90% of optically inactive $[\mathbf{Y_6}]^{2+}$ entities.

Consequently we have synthesized the compound $\{[Eu_6O(OH)_8(NO_3)_2]_{0.05}[Tb_6O(OH)_8(NO_3)_2]_{0.05}[Y_6O(OH)_8(NO_3)_2]_{0.90}(bdc)(Hbdc)_2{\cdot}2NO_3{\cdot}H_2bdc\}_\infty$ hereafter symbolized by $\{[\mathbf{Eu_6}]_{0.05}[\mathbf{Tb_6}]_{0.05}[\mathbf{Y_6}]_{0.90}\}_\infty$. This compound, obtained from a mixture of $[\mathbf{Eu_6}]^{2+}$, $[\mathbf{Tb_6}]^{2+}$, and $[\mathbf{Y_6}]^{2+}$, is isostructural to the other compounds. Tb- and Eu- based homonuclear complexes are statistically isolated. Its luminescence spectrum is reported in Figure 10.

As expected, the emission spectrum of $\{[\mathbf{Eu_6}]_{0.05}[\mathbf{Tb_6}]_{0.05}[\mathbf{Y_6}]_{0.90}\}_\infty$ is nearly the superimposition of

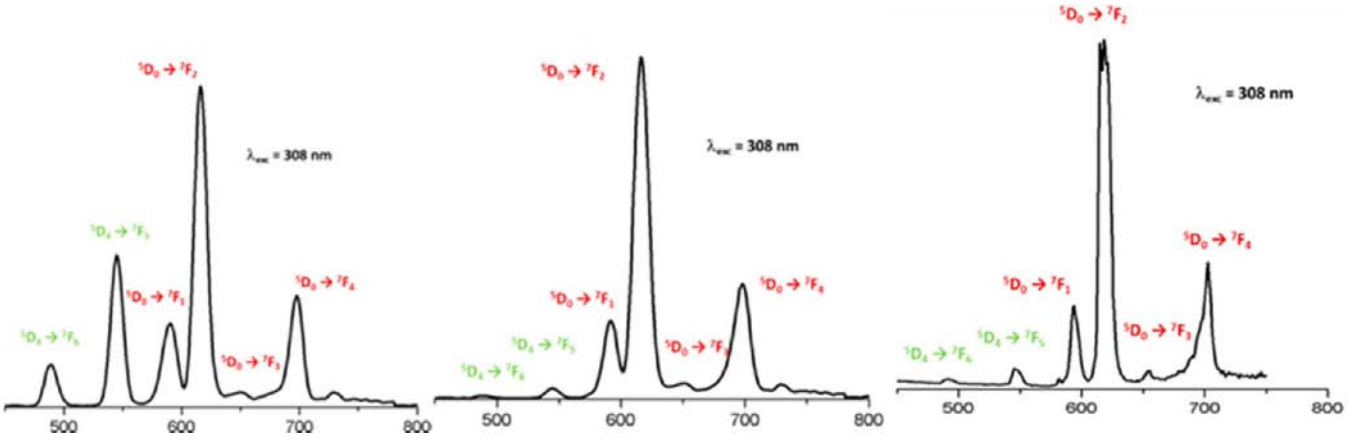

Figure 9. Emission spectra of $\{\mathbf{Eu_6}\}_\infty$ + $\{\mathbf{Tb_6}\}_\infty$ (left), $\{\mathbf{Eu_3Tb_3}\}_\infty$ (center), and $\{[\mathbf{Eu_6}]_{1/2}[\mathbf{Tb_6}]_{1/2}\}_\infty$ (right).

dx.doi.org/10.1021/ic4008697 | Inorg. Chem. 2013, 52, 6720−6730

Scheme 5. Representation of the Energy Transfer in $\{Eu_6\}_\infty$ + $\{Tb_6\}_\infty$ (left) and $\{Eu_3Tb_3\}_\infty$ (right)

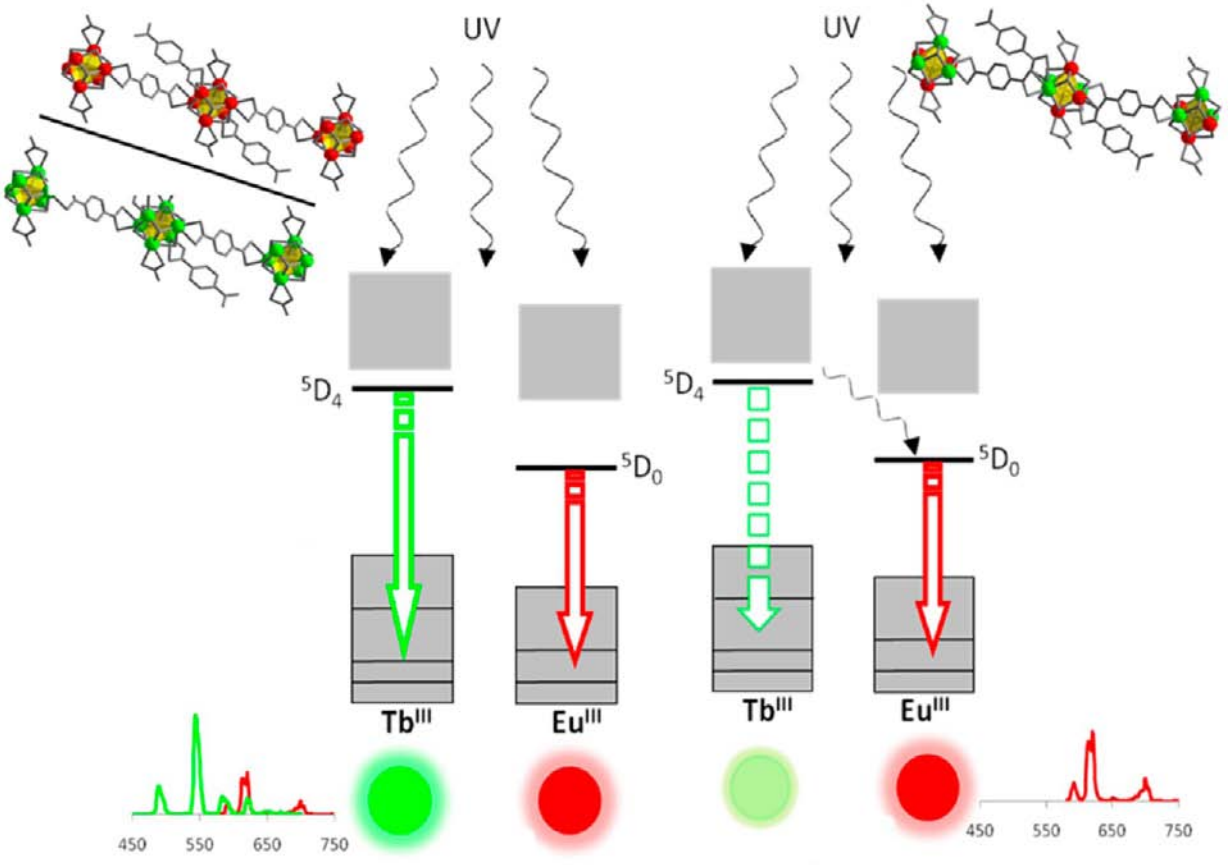

Scheme 6. . Perspective View of the Surrounding of a Central Hexanuclear Complex in a 15 Å Radius Sphere Centered on a μ_6-O Atom[a]

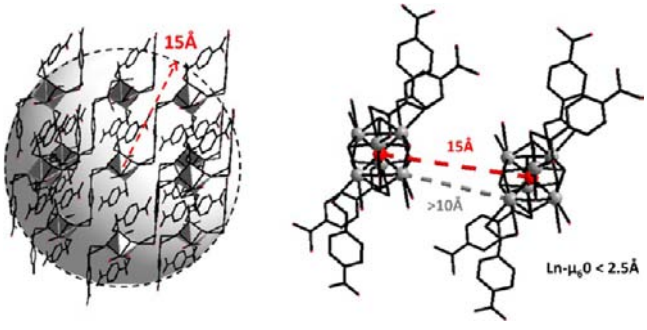

[a]All the lanthanide ions less than 10 Å away from one of the lanthanide ions that belong to the central hexa-nuclear unit are located inside this sphere (Right).

the ones of $\{Eu_6\}_\infty$ and $\{Tb_6\}_\infty$. Actually, it is close to the one of $\{Eu_6\}_\infty$ + $\{Tb_6\}_\infty$. This indicates that in this compound, the hexanuclear complexes are almost isolated and confirms the validity of our approach. Colorimetric measurements have also been performed ($x = 0.52 \pm 1$; $y = 0.44 \pm 1$) and confirm that $\{[Eu_6]_{0.05}[Tb_6]_{0.05}[Y_6]_{0.90}\}_\infty$ colorimetric coordinates are a combination of those of $\{Eu_6\}_\infty$ and $\{Tb_6\}_\infty$ (See Figure 10).

These results also show that, despite a small overall content of optically active lanthanide ions, the solid presents quite high luminance (45 ± 4 Cd m^{-2}). Actually, this study shows that, in contrast with what is observed in "classical" lanthanide-based coordination polymers,[68] dilution of the optically active species by optically non active ones does not affect significantly the brightness of the solid. This is an interesting result as far as the design of highly luminescent material is targeted.

CONCLUSIONS AND OUTLOOK

In this paper we report on a series of hexanuclear complexes-based coordination polymers that exhibit unique luminescent properties. To the best of our knowledge this series of compounds constitutes the first system that presents two different intermetallic energy transfer pathways: The first one (inner energy transfer) occurs inside the hexanuclear units and is similar to intermetallic energy transfers encountered in condensed solids. The second one (outer energy transfer) acts between lanthanides ions belonging to neighboring hexanuclear units and is similar to intermetallic energy transfers observed for hybrids materials. This duality allows a modulation of the luminescence color without affecting the brightness.

These systems are interesting as far as technological applications are targeted. Indeed, playing with the composition of the heterohexanuclear complexes on one hand and with the mixture of different hexanuclear species on the other hand it is possible to achieve the design of highly luminescent and tunable systems at low cost. This is of great interest as far as potential applications in the fight against counterfeiting or for lighting.

From an academic point of view, these systems offer the opportunity of designing systems that would exhibit unique optical properties by playing with energy transfer and up- or

dx.doi.org/10.1021/ic4008697 | Inorg. Chem. 2013, 52, 6720−6730

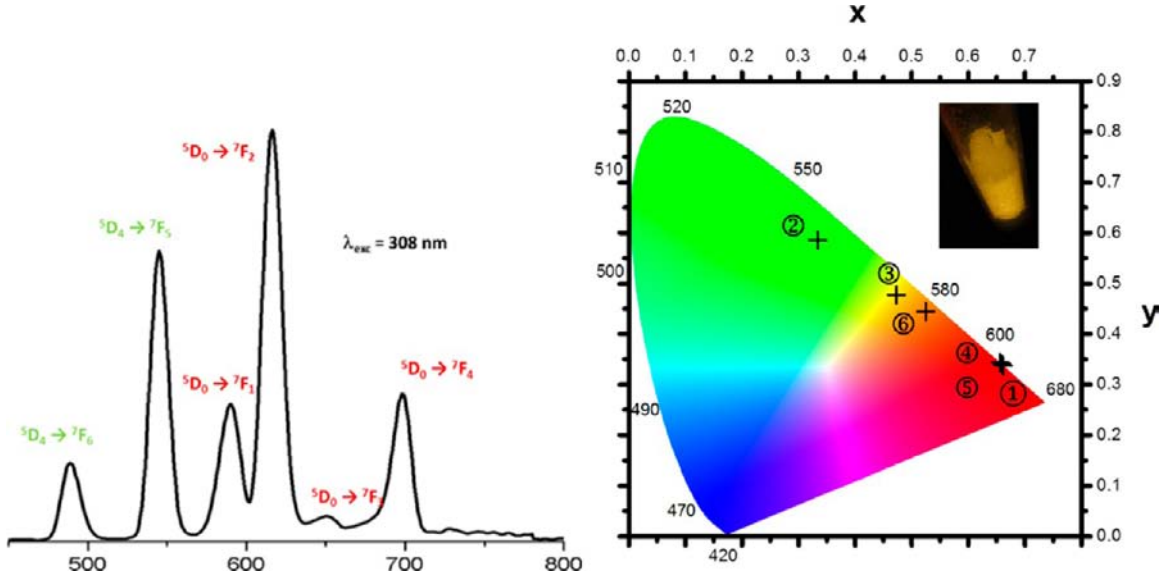

Figure 10. Left: Emission spectrum of $\{[\mathbf{Eu_6}]_{0.05}[\mathbf{Tb_6}]_{0.05}[\mathbf{Y_6}]_{0.90}\}_\infty$. Right: Colorimetric coordinates of $\{\mathbf{Eu_6}\}_\infty$ ①, $\{\mathbf{Tb_6}\}_\infty$ ②, $\{\mathbf{Eu_6}\}_\infty + \{\mathbf{Tb_6}\}_\infty$ ③, $\{\mathbf{Eu_3Tb_3}\}_\infty$ ④, $\{[\mathbf{Eu_6}]_{1/2}[\mathbf{Tb_6}]_{1/2}\}_\infty$ ⑤, and $\{[\mathbf{Eu_6}]_{0.05}[\mathbf{Tb_6}]_{0.05}[\mathbf{Y_6}]_{0.90}\}_\infty$ ⑥. In inset, a picture of $\{[\mathbf{Eu_6}]_{0.05}[\mathbf{Tb_6}]_{0.05}[\mathbf{Y_6}]_{0.90}\}_\infty$ under UV irradiation.

down-conversion inside the heterohexanuclear units and then combining several different such complex nodes in a monophasic hybrid solid.

In this paper, we have demonstrated the validity of this approach. However, the described compounds are not fully optimized and our group is currently working along this line.

■ ASSOCIATED CONTENT

Ⓢ Supporting Information

Selected intermetallic distances in $\{\mathbf{Y_6}\}_\infty$ (Tables S1 and S2). Relative abundance of the different hexanuclear complexes obtained from mixtures of Ln and Ln′ ions (Figure S1); Powder X-ray diffraction diagrams of $\{\mathbf{Eu_6}\}_\infty + \{\mathbf{Tb_6}\}_\infty$, $\{\mathbf{Eu_3Tb_3}\}_\infty$, and $\{[\mathbf{Eu_6}]_{1/2}[\mathbf{Tb_6}]_{1/2}\}_\infty$ (Figure S2). This material is available free of charge via the Internet at http://pubs.acs.org.

■ AUTHOR INFORMATION

Corresponding Author

*E-mail: Olivier.guillou@insa-rennes.fr (O.G.). Phone: (+33) 2 23 23 84 38. Fax: (+33) 2 23 23 87 85. E-mail: guillaume.calvez@insa-rennes.fr (G.C.).

Notes

The authors declare no competing financial interest.

■ ACKNOWLEDGMENTS

Région Bretagne is acknowledged for financial support (ARED Ln6 Program). This research received FEDER financial support (FEDER 34722-Prin^{2}Tan).

■ REFERENCES

(1) Devic, T.; Serre, C.; Audebrand, N.; Marrot, J.; Férey, G. *J. Am. Chem. Soc.* **2005**, *127*, 12788.
(2) Luo, Y.; Calvez, G.; Freslon, S.; Daiguebonne, C.; Roisnel, T.; Guillou, O. *Inorg. Chim. Acta* **2010**, *368*, 170.
(3) Eliseeva, S. V.; Bünzli, J. C. G. *New J. Chem.* **2011**, *35*, 1165.
(4) Eliseeva, S. V.; Bünzli, J. C. G. *Chem. Soc. Rev.* **2010**, *39*, 189.
(5) Bünzli, J. C. G.; Piguet, C. *Chem. Soc. Rev.* **2005**, *34*, 1048.
(6) Bünzli, J. C. G.; Eliseeva, S. V. *Chem. Sci.* **2013**, *4*, 1939−1949.
(7) Lemonnier, J.-F.; Guénée, L.; Beuchat, C.; Wesolowski, T. A.; Mukherjee, P.; Waldeck, D. H.; Gogick, K. A.; Petoud, S.; Piguet, C. *J. Am. Chem. Soc.* **2011**, *133*, 16219.
(8) Eddaoudi, M.; Kim, J.; Rosi, N.; Vodak, D.; Wachter, J.; O'Keeffe, M.; Yaghi, O. M. *Science* **2002**, *295*, 469.
(9) Deng, H.; Doonan, C. J.; Furukawa, H.; Ferreira, R. B.; Towne, J.; Knobler, C. B.; Wang, B.; Yaghi, O. M. *Science* **2010**, *327*, 846.
(10) Fenske, D.; Zhu, N.; Langetepe, T. *Angew. Chem., Int. Ed.* **1998**, *37*, 2640.
(11) Müller, A.; Krickemeyer, E.; Bögge, H.; Schmidtmann, M.; Peters, F. *Angew. Chem., Int. Ed.* **1998**, *37*, 3360.
(12) Weakley, T. J. R. *Inorg. Chim. Acta* **1982**, *63*, 161.
(13) Bernardinelli, G.; Piguet, C.; Williams, A. F. *Angew. Chem., Int. Ed. Engl.* **1992**, *31*, 1622.
(14) Giester, G.; Unfried, P.; Zak, Z. *J. Alloys Compd.* **1997**, *257*, 175.
(15) Unfried, P. *Thermochim. Acta* **1997**, *303*, 119.
(16) Lengauer, C. L.; Giester, G.; Unfried, P. *Powder Diffr.* **1994**, *9*, 115.
(17) Zak, Z.; Unfried, P.; Giester, G. *J. Alloys Compd.* **1994**, *205*, 235.
(18) Unfried, P.; Rossmanith, K. *Monatsh. Chem.* **1992**, *123*, 1.
(19) Unfried, P.; Rossmanith, K.; Blaha, H. *Monatsh. Chem.* **1991**, *122*, 635.
(20) Rossmanith, K.; Unfried, P. *Monatsh. Chem.* **1989**, *120*, 849.
(21) Wang, R.; Selby, H. D.; Liu, H.; Carducci, M. D.; Jin, T.; Zheng, Z.; Anthis, J. W.; Staples, R. J. *Inorg. Chem.* **2002**, *41*, 278.
(22) Zheng, Z. *Chem. Commun.* **2001**, 2521.
(23) Wang, R.; Carducci, M. D.; Zheng, Z. *Inorg. Chem.* **2000**, *39*, 1836.
(24) Zheng, Z.; Wang, R. *Comments Inorg. Chem.* **2000**, *22*, 1.
(25) Baril-Robert, F.; Petit, S.; Pilet, G.; Chastanet, G.; Reber, C.; Luneau, D. *Inorg. Chem.* **2010**, *49*, 10970.
(26) Wang, R.; Liu, H.; Carducci, M. D.; Jin, T.; Zheng, C.; Zheng, Z. *Inorg. Chem.* **2001**, *40*, 2743.
(27) Wang, R.; Zheng, Z.; Jin, T.; Staples, R. J. *Angew. Chem., Int. Ed.* **1999**, *38*, 1813.
(28) Ma, B. Q.; Zhang, D. S.; Gao, S.; Jin, T. Z.; Yan, C. H.; Xu, G. X. *Angew. Chem., Int. Ed.* **2000**, *39*, 3644.
(29) Zheng, X. J.; Jin, L. P.; Gao, S. *Inorg. Chem.* **2004**, *43*, 1600.
(30) Jia, D. X.; Zhang, Y.; Dai, J.; Zhu, Q. Y.; Lu, W.; Guo, W. J. *Inorg. Chem. Commun.* **2005**, *8*, 588.
(31) Weng, D.; Zheng, X.; Jin, L. *Eur. J. Inorg. Chem.* **2006**, 4184.
(32) Park, Y. K.; Choi, S. B.; Kim, H.; Won, B.-H.; Choi, K.; Choi, J. S.; Ahn, W. S.; Won, N. *Angew. Chem., Int. Ed.* **2007**, *46*, 8230.

(33) Ma, S.; Yuan, D.; Wang, X. S.; Zhou, H. C. *Inorg. Chem.* **2009**, *48*, 2072.
(34) Shi, F. N.; Cunha-Silva, L.; Trindade, T.; Paz, F. A. A.; Rocha, J. *Cryst. Growth Des.* **2009**, *9*, 2098.
(35) Liu, J.; Meyers, E. A.; Shore, S. G. *Inorg. Chem.* **1998**, *37*, 5410.
(36) Gandara, F.; Gutierrez-Puebla, E.; Iglesias, M.; Snejko, N.; Monge, M. A. *Cryst. Growth Des.* **2010**, *10*, 128.
(37) Tong, Y. Z.; Wang, Q. L.; Yang, G.; Yang, G. M.; Yan, S. P.; Liao, D. Z.; Cheng, P. *CrystEngComm* **2010**, *12*, 543.
(38) Calvez, G.; Guillou, O.; Daiguebonne, C.; Car, P.-E.; Guillerm, V.; Gérault, Y.; Dret, F. L.; Mahé, N. *Inorg. Chim. Acta* **2008**, *361*, 2349.
(39) Mahé, N.; Guillou, O.; Daiguebonne, C.; Gérault, Y.; Caneschi, A.; Sangregorio, C.; Chane-Ching, J. Y.; Car, P. E.; Roisnel, T. *Inorg. Chem.* **2005**, *44*, 7743.
(40) Calvez, G.; Daiguebonne, C.; Guillou, O.; Pott, T.; Méléard, P.; Le Dret, F. *C. R. Acad. Sci. Paris* **2010**, *13*, 715.
(41) Calvez, G.; Daiguebonne, C.; Guillou, O. *Inorg. Chem.* **2010**, *50*, 2851.
(42) Calvez, G.; Daiguebonne, C.; Guillou, O.; Le Dret, F. *Eur. J. Inorg. Chem.* **2009**, 3172.
(43) Bruno, I. J.; Cole, J. C.; Edgington, P. R.; Kessler, M.; Macrae, C. F.; Mc Cabe, P.; Pearson, J.; Taylo, R. *Acta Crystallogr., Sect. B* **2002**, *B58*, 389.
(44) Allen, F. H. *Acta Crystallograph., Sect. B* **2002**, *B58*, 380.
(45) Dexter, D. L. *J. Chem. Phys.* **1953**, *21*, 836.
(46) Förster, T. *Comparative effects of radiation*; John Wiley & Sons: New York, 1960.
(47) Kerbellec, N.; Kustaryono, D.; Haquin, V.; Etienne, M.; Daiguebonne, C.; Guillou, O. *Inorg. Chem.* **2009**, *48*, 2837.
(48) Kerbellec, N.; Catala, L.; Daiguebonne, C.; Gloter, A.; Stephan, O.; Bünzli, J. C. G.; Guillou, O.; Mallah, T. *New J. Chem.* **2008**, *32*, 584.
(49) Desreux, J. F. In *Lanthanide Probes in Life, Chemical and Earth Sciences*; Choppin, G. R., Bünzli, J. C. G., Eds.; Elsevier: Amsterdam, The Netherlands, 1989; p 43.
(50) Kraus, W.; Nolze, G. *J. Appl. Crystallogr.* **1996**, *29*, 301.
(51) Roisnel, T.; Rodriguez-Carjaval, J. *Mater. Sci. Forum* **2001**, *118*, 378.
(52) Roisnel, T.; Rodriguez-Carjaval, J. In *Proceedings of the Seventh European Powder Diffraction Conference (EPDIC 7)*, Barcelona, Spain, May 20−23, 2000; Materials Science Forum, p 118.
(53) Le Bail, A. *Powder Diffr.* **2004**, *19*, 249.
(54) Shirley, R. In *The CRYSFIRE system for automatic powder indexing*.
(55) Wyszecki, G. In *Handbook of Optics*; Driscoll, W. G., Vaughan, W., Eds.; Mac Graw-Hill Book Company: New York, 1978; p 1.
(56) *International Commission on Illumination−Technical report*; CIE: Vienna, Austria, 1995; Vol. *13-3*.
(57) Kustaryono, D.; Kerbellec, N.; Calvez, G.; Daiguebonne, C.; Guillou, O. *Cryst. Growth Des.* **2010**, *10*, 775.
(58) Zheng, Y.; Kustaryono, D.; Kerbellec, N.; Guillou, O.; Gérault, Y.; Dret, F. L.; Daiguebonne, C. *Inorg. Chim. Acta* **2009**, *362*, 2123.
(59) Qiu, Y.; Daiguebonne, C.; Liu, J.; Zeng, R.; Kerbellec, N.; Deng, H.; Guillou, O. *Inorg. Chim. Acta* **2007**, *360*, 3265.
(60) Luo, Y.; Calvez, G.; Freslon, S.; Bernot, K.; Daiguebonne, C.; Guillou, O. *Eur. J. Inorg. Chem.* **2011**, 3705.
(61) Daiguebonne, C.; Kerbellec, N.; Gérault, Y.; Guillou, O. *J. Alloys Compd.* **2008**, *451*, 372.
(62) Luo, Y.; Bernot, K.; Calvez, G.; Freslon, S.; Daiguebonne, C.; Guillou, O.; Kerbellec, N.; Roisnel, T. *CrystEngComm* **2013**, *15*, 1882.
(63) Luo, Y.; Zheng, Y.; Calvez, G.; Freslon, S.; Bernot, K.; Daiguebonne, C.; Roisnel, T.; Guillou, O. *CrystEngComm* **2013**, *15*, 706.
(64) Daiguebonne, C.; Kerbellec, N.; Guillou, O.; Bünzli, J. C. G.; Gumy, F.; Catala, L.; Mallah, T.; Audebrand, N.; Gérault, Y.; Bernot, K.; Calvez, G. *Inorg. Chem.* **2008**, *47*, 3700.
(65) Binnemans, K. *Chem. Rev.* **2009**, *109*, 4283.
(66) Bünzli, J. C. G. *Acc. Chem. Res.* **2006**, *39*, 53.
(67) Pellé, F.; Surblé, S.; Serre, C.; Millange, F.; Férey, G. *J. Lumin.* **2007**, *122−123*, 492.
(68) Haquin, V.; Etienne, M.; Daiguebonne, C.; Freslon, S.; Calvez, G.; Bernot, K.; Le Polles, L.; Ashbrook, S. E.; Mitchell, M. R.; Bünzli, J. C. G.; Guillou, O. *Eur. J. Inorg. Chem.* **2013**, DOI: 10.1002/ejic.201300381.
(69) Mitchell, M. R.; Carnevale, D.; Orr, R.; Whittle, K. R.; Ashbrook, S. E. *J. Phys. Chem. C* **2012**, *116*, 4273.
(70) Reader, S. W.; Mitchell, M. R.; Johnston, K. E.; Pickard, C. J.; Whittle, K. R.; Ashbrook, S. E. *J. Phys. Chem. C* **2009**, *113*, 18874.
(71) Ashbrook, S. E.; Whittle, K. R.; Lumpkin, G. R.; Farnan, I. *J. Phys. Chem. B* **2006**, *110*, 10358.
(72) Roger, J.; Babizhetsky, V.; Cordier, S.; Bauer, J.; Hiebl, K.; Le Polles, L.; Ashbrook, S. E.; Halet, J. F.; Guerin, R. *J. Solid State Chem.* **2005**, *178*, 1854.
(73) Grinstead, C. M.; Snell, J. L. *Introduction to probability*; American Mathematical Society: Providence, RI, 1997.
(74) Dang, S.; Zhang, J. H.; Sun, Z. M. *J. Mater. Chem.* **2012**, *22*, 8868.